

The Shapes of Things to Come: Probability Density Quantiles

Robert G. Staudte

La Trobe University, Melbourne, Australia, 3086

r.staudte@latrobe.edu.au

14 April, 2016

Abstract

For every discrete or continuous location-scale family having a square-integrable density, there is a unique continuous probability distribution on the unit interval that is determined by the density-quantile composition introduced by Parzen in 1979. These *probability* density quantiles (pdQs) only differ in *shape*, and any two of them can be compared with the Hellinger distance or Kullback-Leibler divergences. In particular the Hellinger distance or root-divergences of pdQs from the class of symmetric distributions on the unit interval are shown to be roughly proportional to the classical third moment skewness coefficient of the pdQ. Further, a more precise classification of shapes by tail behavior is defined in terms of limiting pdQ derivatives at 0 and 1. Convergent empirical estimates of these pdQs are provided. Finally, divergence from, and convergence to, uniformity is investigated.

1 Introduction

The study of shapes of probability distributions is simplified by viewing them through the revealing composition of density with quantile function. Following normalization, the resulting functions are not only location-scale free, but densities of absolutely continuous distributions having the same support. This microcosm of *probability density quantiles* carries essential information regarding shapes and allows for simpler classification by asymmetry and tail weights.

1.1 Background and summary

In the seminal work Parzen (1979) proposed that traditional statistical inference be connected to exploratory data analysis through transformations from standard continuous models (normal, exponential) to the realm of density quantile functions. If the standard models were rejected by goodness-of-fit tests, the next step was nonparametric modeling, with the emphasis on what could be gleaned from sample quantile functions and time series methods. The quantile approach to data analysis was earlier championed by Tukey (1962, 1965, 1977), who also provided insightful commentary into Parzen’s proposals. Further work on quantile-based data modeling can be found in Gilchrist (2000), Parzen (2004) and references therein. Jones (1992) investigates estimation of density quantile functions and their reciprocals, while Ma *et al.* (2011) resolves issues in quantile estimation for discrete distributions.

Here we study the classification of shapes for *probability* density quantiles. While this class is limited by the requirement of square-integrability of the density function, it is rich enough to warrant investigation because the transformation from density to the normalized composition of density function with quantile function removes dependence on location and scale parameters and allows for comparison of shapes of both discrete and continuous models using the Hellinger metric and Kullback-Leibler divergences—with non-trivial and informative results.

In this Section we formally introduce pdQs for continuous distributions and provide numerous examples. The pdQs of discrete distributions are similarly examined in Section 2. Given data, in Section 3 we describe methods for estimating the pdQ’s of discrete and continuous distributions, respectively.

Section 4 contains quantitative measurements of shapes of pdQs. In Section 4.2 we measure asymmetry of the pdQ in terms of its distance from the class of symmetric distributions, using either the Hellinger metric or Kullback-Leibler directed or symmetrized divergences; and, we show they are closely related to the classical skewness coefficient of the pdQ. In Section 4.3 we introduce tail-weight classification in terms of the boundary derivatives of the pdQs.

The ‘shapeless’ uniform distribution is the center of the pdQ universe, as is explained in Section 5, where we also construct a ‘divergence from uniformity’ map for families of distributions and investigate the convergence of repeated applications of the pdQ transformation. Further challenges are posed in Section 6.

1.2 Definitions and properties

Definition 1 Let \mathcal{F} be the class of all right-continuous cumulative distribution functions (cdf's) on the real line. For each $F \in \mathcal{F}$ define the associated left-continuous quantile function of F by $Q(u) \equiv \inf\{x : F(x) \geq u\}$, for $0 < u < 1$. When the random variable X has cdf F , write $X \sim F$. In particular, let $U \sim \mathcal{U}$ where U has the uniform distribution on $[0,1]$. It can be shown, Parzen (1979) for example, that:

1. If $X \sim F \in \mathcal{F}$ and $U \sim \mathcal{U}$, then $Q(U) \sim X$.
2. If $X \sim F \in \mathcal{F}$ and F is continuous, then the composition $FQ(u) \equiv F(Q(u)) = u$, for $0 < u < 1$ and hence $F(X) \sim U$.
3. When $X \sim F$ and $E_F[g(X)]$ exists, by the change of variable $x = Q(u)$

$$E_F[g(X)] = E[gQ(U)] = \int_0^1 gQ(u) du . \quad (1)$$

Special cases are $E_F[X] = \int_0^1 Q(u) du$ and $\text{Var}_F[X] = \int_0^1 \{Q(u) - E[X]\}^2 du$.

4. Let $\mathcal{F}' = \{F \in \mathcal{F} : f = F' \text{ exists and is positive}\}$. For $F \in \mathcal{F}'$ we follow Parzen (1979), Tukey (1965) and define the quantile density function $q(u) = Q'(u) = 1/f(Q(u))$, Its reciprocal $fQ(u)$ is called the density quantile function.

In order to convert density quantiles into probability densities we need to compute:

$$\kappa \equiv E[fQ(U)] = \int f^2(x) dx . \quad (2)$$

Definition 2 For $F \in \mathcal{F}'$, assume $\kappa = E[fQ(U)]$ is finite; that is, f is square integrable. Then one may define the probability density quantile or pdQ of F by $f^*(u) = fQ(u)/\kappa$, $0 < u < 1$. Let $\mathcal{F}'^* \subset \mathcal{F}'$ denote the class of all such F .

Not all densities are square integrable, and for such densities a pdQ does not exist. Examples are the Chi-squared densities with degrees of freedom $\nu \leq 1$. Others are the Beta(a, b) densities with $a \leq 1/2$ or $b \leq 1/2$.

An important property of pdQs is that they are location-scale invariant. For if $F_{a,b}(\cdot) \equiv F(\cdot - a)/b$ for arbitrary a and $b > 0$, defines the location-scale family generated by $F = F_{0,1} \in \mathcal{F}$, then the quantile function for $F_{a,b}$ is $Q_{a,b}(u) = a + bQ(u)$. Further, if $F \in \mathcal{F}'$ the quantile density is $q_{a,b}(u) = bq(u)$; thus the quantile density is location-invariant and scale equivariant. Clearly $f_{a,b}^*$ is also scale invariant, and one can write $f_{a,b}^* = f_{0,1}^* = f^*$. Thus when comparing the graphs of different f^* s, we are comparing only their shapes.

Conversely, given an $f^* \in \mathcal{F}'^*$, one can identify the family $\{F_{a,b} : a, b > 0\}$. For if it is known that f^* has the form $f^* = \kappa(fQ)$, for some unknown F with associated $f = F'$, Q , $q = 1/(fQ)$ and κ , then one can reconstruct $Q(u) = \int_0^u q(t) dt + c = \kappa \int_0^u \{f^*(t)\}^{-1} dt + c$; thus Q is determined up to location and scale, as is F . An open question is whether, given an arbitrary continuous distribution with probability density g on $(0, 1)$, does there exist an $F \in \mathcal{F}'$ such that $g = f^*$?

Another property of pdQs is that they ignore flat spots in F . For example, the pdQ f_{gap}^* of $f_{\text{gap}}(x) = (e^x/2) I_{(-\infty, 0]}(x) + I_{[1/2, 1]}(x)$ is the same as that of $f(x) = (e^x/2) I_{(-\infty, 0]}(x) + I_{[0, 1/2]}(x)$. Thus it is only the shape of the distribution on its support that is captured by the pdQ.

1.3 Examples of continuous pdQs

Unless otherwise noted we follow standard definitions for cdf s as described in Johnson *et al.* (1994, 1995). Many of the pdQs $f^*(u) = fQ(u)/\kappa$ discussed in this section are merely normalized versions of density quantiles fQ described in Parzen (1979).

For the normal distribution Φ with density φ , we write $z_u = \Phi^{-1}(u)$ and then it has $\varphi^*(u) = 2\sqrt{\pi}\varphi(z_u)$. Its graph is shown in the upper left plot of Figure 1. It is quite close to that of a quadratic function which is symmetric about $1/2$ and passes through $(0,0)$ and $(1/2, \sqrt{2})$, and not unlike the exact quadratic $f^*(u) = 6u(1-u)$ corresponding to the logistic distribution. The U-shaped Beta(2/3,2/3) distribution retains its U-shape, and the bell-shaped Cauchy retains a bell-shape after transformation to the quantile scale. The Laplace (double-exponential) family transforms to the symmetric triangular distribution.

The Tukey(λ) family of distributions is defined by its quantile function $Q_\lambda(u) = \{u^\lambda - (1-u)^\lambda\}/\lambda$ for $\lambda \neq 0$ and $Q_0(u) = \ln(u/(1-u))$, but in general no closed form expression is available for its density. For $\lambda > 0$ the density has finite support $[-1/\lambda, +1/\lambda]$, and otherwise has infinite support. It has pdQ $f_\lambda^*(u) = 1/\{Q'_\lambda(u)\kappa_\lambda\} = \{u^{\lambda-1} + (1-u)^{\lambda-1}\}^{-1}/\kappa_\lambda$. The constant κ_λ required to make $\int f_\lambda^*(u) = 1$ can be obtained by numerical integration but a good approximation is given by:

$$\kappa_\lambda \approx \begin{cases} \frac{3\lambda}{6}, & \lambda \leq 1; \\ \frac{\lambda}{2}, & 1 \leq \lambda \leq 2; \\ \left(\frac{2}{\pi}\right)^{\lambda-2}, & 2 \leq \lambda \leq 6. \end{cases} \quad (3)$$

For $\lambda \leq 2$ the absolute error of this approximation is less than 0.005, and for $2 \leq \lambda \leq 6$ it is less 0.1. The absolute relative error of approximation is less than 0.06 for $-1 \leq \lambda \leq 6$. The f_λ^* s take on many shapes (not shown in Figure 1.)

The Pareto families (Type I or II) with shape parameter $a > 0$ have pdQs defined by $f_a^*(u) = (2 + 1/a)(1-u)^{1+1/a}$. As $a \rightarrow \infty$ the graphs of f_a^* rapidly approach a triangle, the graph of the exponential distribution pdQ. The remaining graphs in Figure 1 are 3:1 mixtures of two normal distributions; Mixture 1 has components $N(0,1)$ and $N(3,1)$, and Mixture 2 components are $N(0,1)$ and $N(3,1/4^2)$

These examples provide us with some markers when working on the domain $(0,1)$ of the pdQs. All uniform densities transform to the standard uniform pdQ; bell-shaped densities with short tails transform to densities defined roughly by quadratic functions; and exponential distributions correspond to triangular shapes. Finally, mixtures of normal densities appear to transform to a ‘mixture of quadratics’.

A larger class of pdQs are generated by the *generalized lambda* family, which we return to in Section 5.1. It has quantile function determined by a location parameter λ_1 , an inverse scale parameter $\lambda_2 > 0$ and two shape parameters λ_3 and λ_4 :

$$Q(u) = \lambda_1 + \frac{1}{\lambda_2} \left\{ \frac{u^{\lambda_3} - 1}{\lambda_3} - \frac{(1-u)^{\lambda_4} - 1}{\lambda_4} \right\}. \quad (4)$$

This is called the FKML parameterization, after Freimer *et al.* (1988). In deriving its pdQ we can without loss of generality assume $\lambda_1 = 0$ and $\lambda_2 = 1$.

The *quantile density* is $q_{\lambda_3, \lambda_4}(u) = u^{\lambda_3-1} + (1-u)^{\lambda_4-1}$, so its reciprocal, the density quantile, is given for each $0 < u < 1$ by

$$(fQ)_{\lambda_3, \lambda_4}(u) = \{u^{\lambda_3-1} + (1-u)^{\lambda_4-1}\}^{-1}. \quad (5)$$

Then the pdQ of f is given by $f_{\lambda_3, \lambda_4}^*(u) \equiv (fQ)_{\lambda_3, \lambda_4}(u)/\kappa$, where the normalizing constant is obtained by numerical integration.

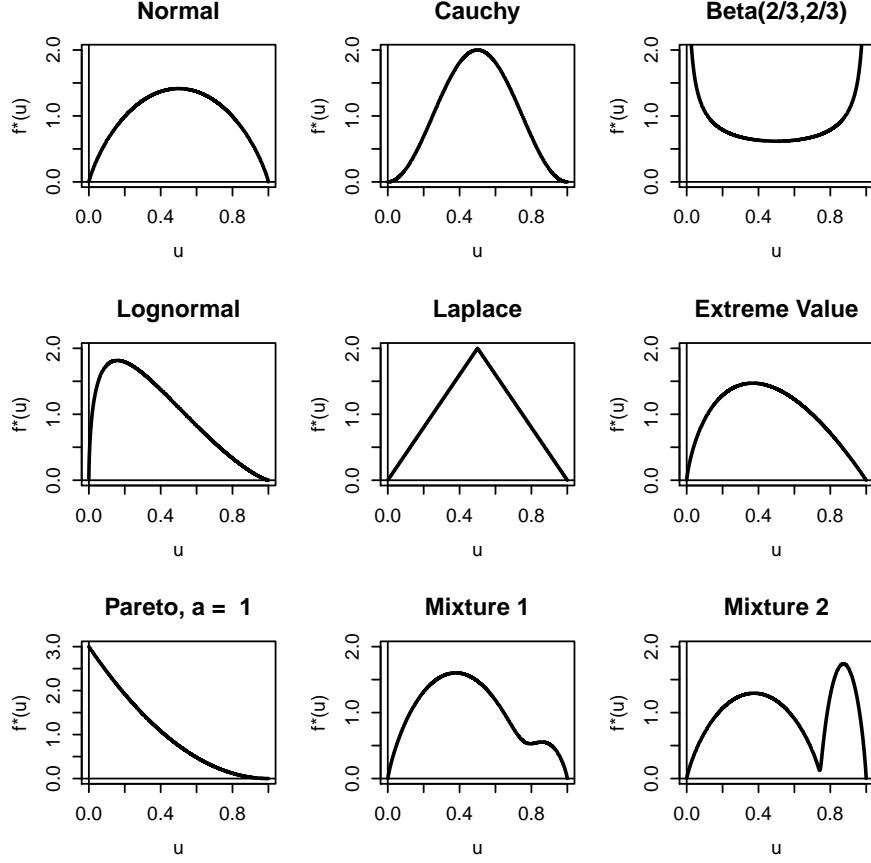


Figure 1: **pdQs of some continuous distributions.** Details are given in Section 1.3.

Table 1: **Examples of distributions F and associated quantile functions and pdQs.** In general, we denote $x_u = Q(u) = F^{-1}(u)$, but for the normal $F = \Phi$ with density φ , we write $z_u = \Phi^{-1}(u)$. The power function distribution is also known as the Beta($b, 1$) family. For the Weibull(β) family, no simple approximation for κ_β is available. Similarly for the Tukey(λ) family, κ_λ is not available, but a simple approximation is given in Section 1.3.

| | $1 - F(x)$ | $Q(u)$ | $f^*(u)$ |
|--------------------|---|---|---|
| Power(b) | $1 - x^b, 0 < x < 1$ | $u^{1/b}$ | $(2 - \frac{1}{b})u^{1-1/b}, b > 1/2$ |
| Laplace | $1 - e^x/2, x \leq 0$ $e^{-x}/2, x \geq 0$ | $\ln(2u), u \leq 0.5$ $-\ln(2(1-u)), u \geq 0.5$ | $2 \min\{u, 1-u\}$ |
| Logistic | $(1 + e^x)^{-1}$ | $\ln(u/(1-u))$ | $6u(1-u)$ |
| Extreme Value | $1 - e^{-e^{-x}}$ | $-\ln(-\ln(u))$ | $-4u \ln(u)$ |
| Cauchy | $\frac{1}{2} - \frac{1}{\pi} \arctan(x)$ | $\tan\{\pi(u - 0.5)\}$ | $2 \sin^2(\pi u)$ |
| Tukey(λ) | — | $\frac{u^\lambda - (1-u)^\lambda}{\lambda}$ | $\{\kappa_\lambda (u^{\lambda-1} + (1-u)^{\lambda-1})\}^{-1}$ |
| Normal | $\Phi(-x)$ | z_u | $2\sqrt{\pi} \varphi(z_u)$ |
| Lognormal | $\Phi(-\ln(x))$ | e^{z_u} | $\frac{2\sqrt{\pi}}{e^{1/4}} \varphi(z_u) e^{-z_u}$ |
| Pareto(a) | $x^{-a}, x \geq 1$ | $(1-u)^{-1/a}$ | $(2 + \frac{1}{a})(1-u)^{1+1/a}$ |
| Exponential | $e^{-x}, x \geq 0$ | $-\ln(1-u)$ | $2(1-u)$ |
| Weibull(β) | $e^{-x^\beta}, x \geq 0$ | $\{-\ln(1-u)\}^{1/\beta}$ | $\frac{\beta(1-u)}{\kappa_\beta \{-\ln(1-u)\}^{1/\beta-1}}$ |

Table 2: Mean, standard deviation, and coefficients of skewness and kurtosis of some pdQs. Clearly $\mu^* = 0.5$ and $\gamma_1^* = 0$ in the symmetric case.

| F | σ^* | γ_2^* | F | μ^* | σ^* | γ_1^* | γ_2^* |
|---------------|------------|--------------|---------------|---------|------------|--------------|--------------|
| Beta(2/3,2/3) | 0.3561 | 1.4846 | Pareto(0.5) | 0.2000 | 0.1633 | 1.0498 | 3.6964 |
| Uniform | 0.2887 | 1.8000 | Pareto(1) | 0.2500 | 0.1936 | 0.8607 | 3.0952 |
| Laplace | 0.2041 | 2.4000 | Pareto(2) | 0.2857 | 0.2130 | 0.7318 | 2.7566 |
| Cauchy | 0.1808 | 2.4062 | Weibull(2) | 0.4557 | 0.2393 | 0.1315 | 2.0714 |
| t_2 | 0.2041 | 2.2500 | χ_2^2 | 0.3333 | 0.2357 | 0.5657 | 2.4000 |
| t_3 | 0.2131 | 2.1961 | χ_3^2 | 0.3849 | 0.2354 | 0.3808 | 2.2246 |
| t_5 | 0.2207 | 2.1527 | χ_5^2 | 0.4205 | 0.2343 | 0.2618 | 2.1513 |
| t_7 | 0.2240 | 2.1341 | χ_7^2 | 0.4358 | 0.2337 | 0.2116 | 2.1291 |
| Normal | 0.2326 | 2.0878 | Lognormal | 0.3415 | 0.2165 | 0.5487 | 2.5035 |
| Logistic | 0.2236 | 2.1429 | Extreme Value | 0.4444 | 0.2291 | 0.1872 | 2.1459 |

1.4 Moments of pdQs

Let $X^* \sim f^*$ and define $\mu_k^* = E[(X^*)^k] = \kappa^{-1} \int u^k fQ(u) du = \kappa^{-1} \int F^k(x) f^2(x) dx$. All moments of X^* exist because it is bounded. Denote the mean of X^* by μ^* , the standard deviation by σ^* and the classical moment based coefficients of skewness and kurtosis by γ_1^* and γ_2^* . Some examples, obtained numerically, are shown in Table 2. For all the distributions in Table 1, γ_1^* is a good linear predictor of the Hellinger distance of f^* from the class of symmetric distributions on $[0,1]$, as we will see in Section 4.2.

2 Discrete pdQs

Let $\mathcal{X} = \{x_i\}$ denote a finite or infinite sequence of distinct real numbers and let $\{p_i\}$ be an associated sequence of positive numbers whose sum is one. Then $\{(x_i, p_i)\}$ defines a *discrete probability distribution*. The class of such distributions is too rich to meaningfully discuss shape via pdQs, so we restrict \mathcal{X} to a *lattice*, a sequence of equally spaced points. By a location-scale change this can always be taken to be a subset of the integers. For most distributions of interest to us this domain is a finite set of the form $\{0, 1, \dots, n\}$ or $\{0, 1, 2, \dots\}$. Let $\mathcal{D} \subset \mathcal{F}$ be the set of all lattice distributions; they are comprehensively treated by Johnson *et al.* (1993).

Definition 3 The cdf of each $F \in \mathcal{D}$ is defined for all real x by $F(x) = \sum_{j \leq x} p_j$. This monotone increasing F is a right-continuous step function with jumps of size p_i at each i , and hence value $F(x) = S_i = \sum_{j \leq i} p_j$ for x lying in $[i, i+1)$. The quantile function Q of $F \in \mathcal{D}$ is a monotone increasing left-continuous step function with value i for u lying in $(S_{i-1}, S_i]$. The discrete density quantile function $pQ(u)$ is therefore a step function with value p_i for u lying in $(S_{i-1}, S_i]$. In general, the graph of pQ covers a sequence of adjacent squares with respective sides equal to p_i . Since the sum of the areas of these squares $\kappa = \sum_i p_i^2$ is finite, we can define the discrete probability density quantile by $p^*(u) = pQ(u)/\kappa$. Given p^* , one can recover $\{p_i\}$.

Note that a discrete distribution $\{p_i\}$ on a lattice is transformed by this composition and normalization into p^* , which is the density with respect to Lebesgue measure of a continuous distribution with support $[0,1]$. It is a normalized histogram that captures the shape of the original discrete distribution on its support, free of location and scale. When there is no chance of confusion we may write f^* for p^* .

In Figure 2 are shown pdQs for some Poisson(λ) distributions. Note that as λ increases, the shapes of these graphs approach that of the normal pdQ, earlier depicted in the upper left plot of Figure 1.

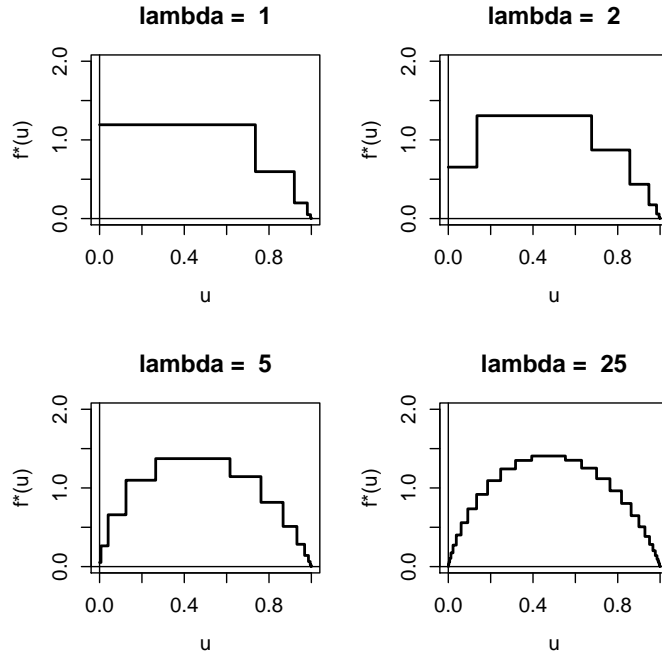


Figure 2: pdQs of some Poisson distributions.

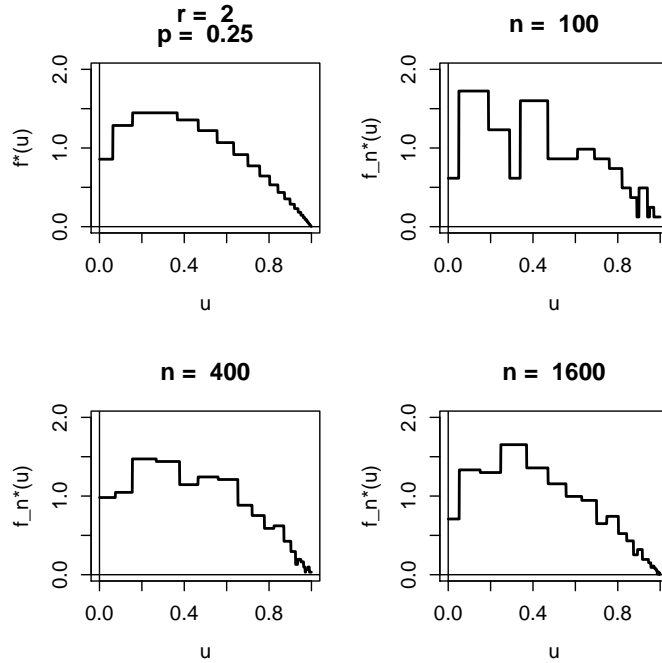


Figure 3: pdQ of the negative binomial distribution with parameters $r = 2$, $p = 0.25$. The remaining empirical pdQ plots are based on (6), using random samples of size n from this distribution.

3 Empirical pdQs

Given a sample of data from an unknown $F \in \mathcal{F}$, we want to estimate its pdQ. This will be done separately for the discrete $F \in \mathcal{D}$ and continuous $F \in \mathcal{F}'$ cases.

3.1 An empirical pdQ for a sample from $F \in \mathcal{D}$

Given n real numbers which have $M \leq n$ distinct values $x_1 < x_2 < \dots < x_M$, let $f_n(x_m)$ be the relative frequency of occurrences of x_m ; that is, $f_n(x_m) = n_m/n$ for each $m = 1, \dots, M$ where each $1 \leq n_m \leq n$ and $\sum_m n_m = n$. Let $c_n(m) = (\sum_{j=1}^m n_j)/n$. It follows that the empirical cdf is of the form:

$$F_n(x) = \begin{cases} 0, & \text{for } x < x_1 ; \\ c_n(m), & \text{for } x_m \leq x < x_{m+1} ; \\ 1, & \text{for } x_M \leq x . \end{cases}$$

The associated empirical quantile function Q_n jumps by amount $f_n(x_m)$ at the point $c_n(m) = F_n(x_m)$, for $m = 1, \dots, M-1$, and is otherwise flat.

$$Q_n(u) = x_m, \text{ for } c_n(m-1) < u \leq c_n(m), \quad m = 1, \dots, M-1 .$$

Definition 4 Letting $c_n(0) = 0$, define for each $0 < u < 1$ the empirical density quantile to be the step function:

$$f_n Q_n(u) = \sum_{m=1}^M \frac{n_m}{n} I\{c_n(m-1) < u \leq c_n(m)\} . \quad (6)$$

To make this a probability density quantile, it needs to be divided by

$$\kappa_n = \int_0^1 f_n Q_n(u) du = \frac{1}{n^2} \sum_{m=1}^M n_m^2 .$$

The empirical pdQ is therefore given for each $0 < u < 1$ by:

$$f_n^*(u) = \frac{n \sum_{m=1}^M n_m I\{c_n(m-1) < u \leq c_n(m)\}}{\sum_{m=1}^M n_m^2} . \quad (7)$$

If all n observations are distinct, this empirical pdQ is identically one, just as it is for any other discrete or continuous uniform distribution.

As an example, the top left plot of Figure 3 shows the graph of the pdQ of the negative binomial distribution with $r = 2$ and $p = 1/4$. The other plots show empirical pdQs, based on random samples of varying sample sizes.

3.2 An empirical pdQ for a sample from $F \in \mathcal{F}'$

For smooth distributions $F \in \mathcal{F}'$ we propose estimating $q(u)$ by the estimator already studied by many authors, including Falk (1986), Welsh (1988) and Jones (1992). It is the kernel density estimator that can be written as a linear combination of order statistics:

$$\hat{q}_n(u) = \sum_{i=1}^n X_{(i)} \left\{ k_b \left(u - \frac{(i-1)}{n} \right) - k_b \left(u - \frac{i}{n} \right) \right\}, \quad (8)$$

where b is a bandwidth and $k_b(\cdot) = \frac{1}{b} k(\cdot/b)$ for some kernel k which is an even function on $[-1, 1]$ that has variance $\sigma_k^2 = \int x^2 k(x) dx$ and roughness $r_k = \int k^2(y) dy$. It

turns out that the asymptotic mean squared error of $\hat{q}(u)$ is minimized when the bandwidth

$$b(u) = \left(\frac{r_k}{n \sigma_k^4} \right)^{1/5} \left\{ \frac{q(u)}{q''(u)} \right\}^{2/5}. \quad (9)$$

For the Epanechnikov (1969) kernel, the first factor in this expression reduces to $(15/n)^{1/5}$. Thus the asymptotically optimal choice of bandwidth (9) for estimating $q(u)$ only depends on the underlying distribution through the quantile optimality ratio $\text{QOR}(u) = q(u)/q''(u)$, which is location and scale invariant. Prendergast & Staudte (2016) show that for many examples the graph of the QOR is very similar in shape to the density quantile $fQ(u) = 1/q(u)$, and hence remarkably stable for F in broad classes such as all symmetric unimodal distributions, or all F with positive unimodal density on $[0, +\infty)$. Further, they show that by employing the Cauchy QOR, one obtains good estimators $\hat{q}(u)$ of $q(u)$ for all F in the first class, while the optimal QOR for the lognormal yields good estimators for all F in the second. An R script for implementing these estimators is provided in accompanying online material. In Figure 4 are shown examples of the graphs of $f^*(u) = 1/\{\kappa q(u)\}$ and the estimators $f_m^*(u) = 1/\{\hat{\kappa} \hat{q}_n(u)\}$, $u = 0.005 : 0.995/0.01$, for sample size $n = 1600$. Smaller sample sizes as low as 400 provide a rough idea of the shape.

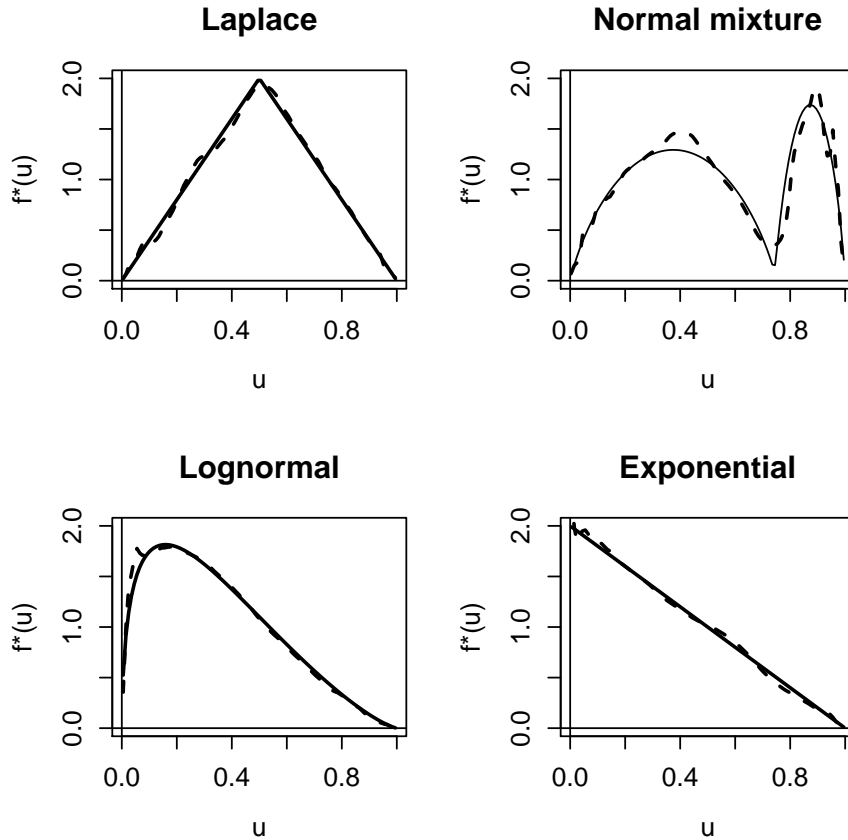


Figure 4: Graphs of $f^*(u)$ (solid lines) and their estimates (dashed lines). The normal mixture puts weights $3/4, 1/4$ on the standard normal Φ and $\Phi((\cdot - 3)/(1/4))$ respectively. The optimal QOR for the Cauchy as used in the top two plots, while the optimal QOR for the lognormal in the others.

4 Numerical measures of shapes of pdQs

An advantage of working with f^* s over f s is that they have the same bounded support $[0, 1]$. Therefore the classical skewness and kurtosis measures are always defined, with examples for continuous families in Table 2. A similar table could be constructed for discrete distributions. Moreover the pdQs for both discrete and continuous F are densities with respect to Lebesgue measure and have the same support, so in particular the Kullback-Leibler symmetrized divergence between the pdQs of discrete and continuous distributions is non-degenerate. For example, let $0 < r \leq 1$, $X \sim \text{Exponential}(\lambda)$ with $\lambda = 1$ and $Y_r = \lfloor rX \rfloor \sim \text{Geometric}(p_r)$, with $p_r = 1 - e^{-r}$. Then the Hellinger distance of X^* from Y_r^* is $H_r \approx r/10$; and the root-KLD divergence $\sqrt{J_r} \approx 3r/11$, for $0 < r \leq 1$.

In addition to skewness and kurtosis of pdQs, the ‘shape’ can be described by the number and location of modes, and the tail behavior of f^* at 0 and 1.

4.1 Divergence and distance measures

Given probability distributions having densities f_1, f_2 with respect to Lebesgue measure, the *Hellinger distance* $H(f_1, f_2)$ between them is defined by

$$H(f_1, f_2) = \left[\frac{1}{2} \int \left\{ \sqrt{f_1(x)} - \sqrt{f_2(x)} \right\}^2 dx \right]^{1/2}. \quad (10)$$

The Hellinger distance satisfies the properties of any other metric: non-negativity, equalling zero if and only if $f_1 = f_2$ almost everywhere, symmetry, and sub-additivity (the triangle inequality). A *semi-metric* satisfies all the properties of a metric except sub-additivity.

The *Kullback-Leibler information* $I(f_1 : f_2)$ in $X \sim f_1$ for discrimination between f_1, f_2 is defined by (Kullback, 1968, p.5) as

$$I(f_1 : f_2) = \int \ln \left\{ \frac{f_1(x)}{f_2(x)} \right\} f_1(x) dx. \quad (11)$$

As explained by (Kullback, 1968, p.5), the log-likelihood $\ln\{f_1(x)/f_2(x)\}$ can also be interpreted as the *evidence* for f_1 over f_2 in data x , so $I(f_1 : f_2)$ is the average evidence for f_1 over f_2 in one observation $X \sim f_1$. (Kullback, 1968, p.14) show that $I(f_1 : f_2) \geq 0$ with equality if and only if $f_1 = f_2$ almost everywhere. The *Kullback-Leibler symmetrized divergence* KLD, is defined by $J(1, 2) = I(1 : 2) + I(2 : 1)$. It satisfies all properties of a metric except the triangle inequality, and is thus a semi-metric, by definition.

In the sequel we will often abbreviate $H(f_1, f_2)$ to $H(1, 2)$, $I(f_1 : f_2)$ to $I(1 : 2)$ and $J(f_1, f_2)$ to $J(1, 2)$. Further, we denote by $H^*(1, 2)$ the Hellinger metric applied to the pdQs f_1^*, f_2^* of f_1, f_2 , and similarly for $I^*(1 : 2)$ and $J^*(1, 2)$.

4.2 Finding the closest symmetric distribution to a pdQ

One can measure the skewness of a pdQ using the classical moment-based quantity as found in Table 2, as well as many other definitions, see for example Staudte (2014). But skewness is just one aspect of asymmetry, for an asymmetric distribution can have zero skewness. We will measure the asymmetry of a pdQ by finding its Hellinger distance or divergence to the closest symmetric distribution.

It is shown in Theorem 3.2 of Withers & Nadarajah (2010) that if f_1, f_2 are densities with respect to Lebesgue measure and f_2 is assumed to be symmetric about 0, then the closest such f_2 to f_1 in terms of minimizing the Hellinger distance is given by $f_2(x) = \alpha^2(x)/d$ where $\alpha(x) = \{\sqrt{f_1(x)} + \sqrt{f_1(-x)}\}/2$ and $d = 2 \int_0^{+\infty} \alpha^2(x) dx$.

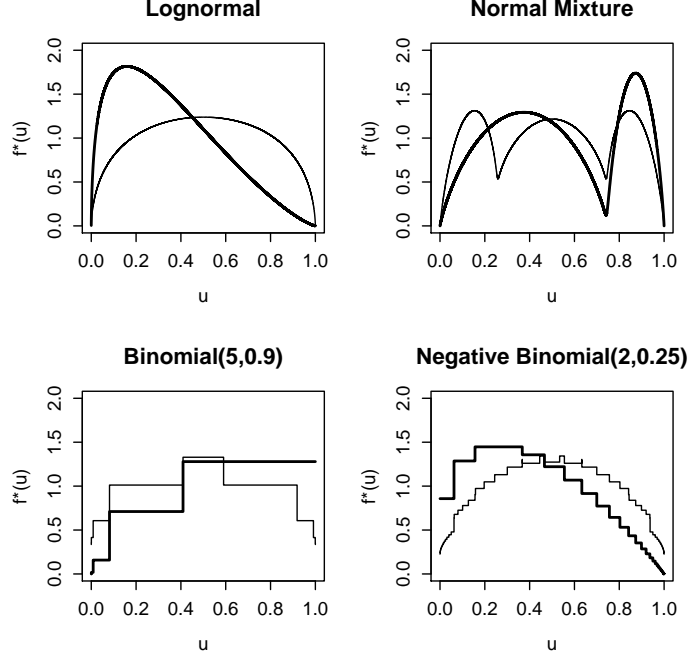


Figure 5: Graphs of $f^*(u)$ in thick black lines and their respective closest (in the Hellinger distance) symmetric distributions f_{symm}^* in thin lines. The normal mixture puts weights $3/4, 1/4$ on the standard normal Φ and $\Phi((\cdot - 3)/(1/4))$ respectively. The respective Hellinger distances to the symmetric class in the four cases are 0.2386 , 0.1255 , 0.1376 and 0.1443 .

Consequently, if f^* is an arbitrary pdQ, the Hellinger-closest symmetric distribution is given by $f_{\text{symm}}^*(u) = \alpha^2(u)/d$ where $\alpha(u) = \{\sqrt{f^*(u)} + \sqrt{f^*(1-u)}\}/2$ and $d = \int_0^1 \alpha^2(u) du$. The actual Hellinger distance $H_{\min}(f^*) = H(f^*, f_{\text{symm}}^*)$ of f^* from the class of symmetric distributions is determined by:

$$2\{1 - H_{\min}^2(f^*)\}^2 = 1 + \int_0^1 \sqrt{f^*(u)f^*(1-u)} du. \quad (12)$$

Some examples are shown in Figure 5. As an aside, the closest symmetric density to the extreme value pdQ differs from the normal pdQ by no more than 0.01.

Withers & Nadarajah (2010) also find the closest symmetric distribution to a given one in the sense of minimizing the Kullback-Leibler divergence (11). Their result is extended to minimizing $J(1, 2)$ as follows.

Proposition 1 *Given f_1, f_2 probability densities with respect to Lebesgue measure, and assume that f_2 is symmetric about 0. Then*

- (a) *The f_2 that minimizes $I(2 : 1)$ is given by $f_2(x) = \nu(x)/d$, where $\nu(x) = \sqrt{f_1(x)f_1(-x)}$ and $d = 2 \int_0^{+\infty} \nu(x) dx$.*
- (b) *The f_2 that minimizes $I(1 : 2)$ is given by $f_2(x) \equiv \bar{f}_1(x) \equiv \{f_1(x) + f_1(-x)\}/2$.*
- (c) *The f_2 that minimizes $J(1, 2)$ is given by $f_2(x) = \beta(x)/d$ where $\beta(x)$ is the solution to:*

$$\beta(x) = \nu(x) \exp \{\bar{f}_1(x)/\beta(x)\}; \quad (13)$$

and $d = 2 \int_0^\infty \beta(x) dx$.

The proof of Proposition 1 is in the Appendix 7.1, along with an algorithm for computing the minimizer of J guaranteed by Part (c), plus two illustrative examples.

In our applications of Proposition 1 to pdQs the support of f_1 and f_2 is the unit interval, and symmetry takes place about $1/2$, so $\bar{f}_1(x) \equiv \{f_1(x) + f_1(-x)\}/2$ becomes $\bar{f}_1(u) \equiv \{f_1(u) + f_1(1-u)\}/2$, and similarly for $\nu(x)$.

Table 3: **Examples of measures of asymmetry for pdQs.** For each F with density f is shown the moment coefficient of skewness γ_1^* of f^* taken from Table 1, the minimum Hellinger distance $H^* = H_{\min}(f^*)$ determined by (12), and similarly the respective minimum divergences $I_{1:}^*$, $I_{:1}^*$ and J^* to the class of symmetric densities described in Proposition 1.

| F | γ_1^* | H^* | $I_{1:}^*$ | $I_{:1}^*$ | J^* |
|---------------|--------------|--------|------------|------------|--------|
| Pareto(0.5) | 1.0498 | 0.4421 | 0.5401 | 1.2224 | 2.1589 |
| Pareto(1) | 0.8607 | 0.3660 | 0.4077 | 0.6931 | 1.2710 |
| Pareto(2) | 0.7318 | 0.3094 | 0.3107 | 0.4535 | 0.8507 |
| Weibull(2) | 0.1315 | 0.0672 | 0.0178 | 0.0182 | 0.0363 |
| χ_2^2 | 0.5657 | 0.2349 | 0.1931 | 0.2416 | 0.4646 |
| χ_3^2 | 0.3808 | 0.1687 | 0.1061 | 0.1191 | 0.2326 |
| χ_5^2 | 0.2618 | 0.1191 | 0.0548 | 0.0580 | 0.1145 |
| χ_7^2 | 0.2116 | 0.0970 | 0.0368 | 0.0382 | 0.0757 |
| Lognormal | 0.5487 | 0.2386 | 0.2014 | 0.2500 | 0.4747 |
| Extreme Value | 0.1872 | 0.0855 | 0.0287 | 0.0295 | 0.0587 |

In Table 3 are listed the values of some possible measures of asymmetry for a given pdQ f^* for f belonging to an asymmetric location-scale family F . These values are positively correlated, and γ_1^* , H^* , $\sqrt{I_{1:}^*}$, $\sqrt{I_{:1}^*}$ and $\sqrt{J^*}$ are very highly correlated, as shown in Figure 6.

To show that $H^* = 0.43 \times |\gamma_2^*|$ is only an approximation on the class of pdQs, consider the power function family $F_b(u) = u^b$, $0 < u < 1$, $b > 0$, which is also the Beta($b, 1$) family. Assuming $b > 1/2$, it has pdQ $f_b^* = f_{b^*}$ with $b^* = 2 - 1/b$, so $f_b^* \sim \text{Power}(b^*)$, or Beta($b^*, 1$). The skewness coefficient of the Beta family is known (Johnson *et al.*, 1995, p.217), and in this case $\gamma_1(b^*) = 2(1 - b^*)\sqrt{1 + 2/b^*}/(b^* + 3)$, for $\beta^* \in (0, 2]$. It is monotone decreasing in b^* over this range with limiting values $\gamma_1(0+) = +\infty$ and $\gamma_1(2) = -2\sqrt{2}/5$.

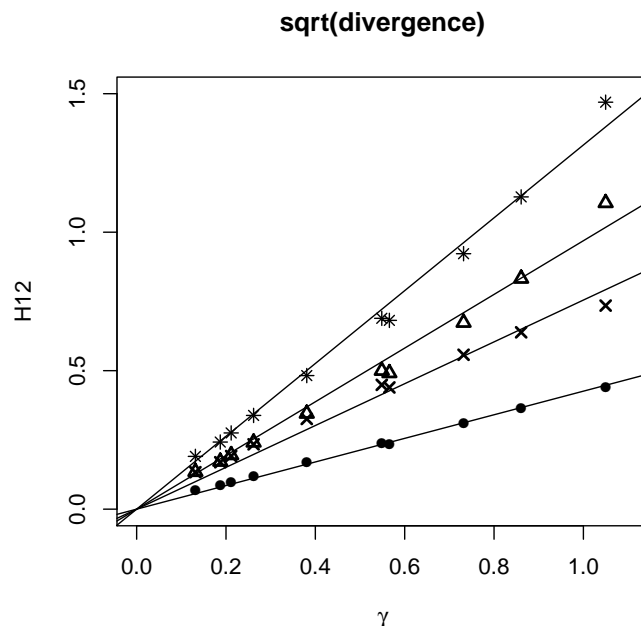


Figure 6: Plots of H^* versus $\gamma = \gamma_1^*$ in circles, and $\sqrt{I_{1:}^*}$, $\sqrt{I_{:1}^*}$ and $\sqrt{J^*}$ against γ in crosses, triangles and asterisks, respectively, based on results in Table 3. Superimposed are their least-squares lines through the origin, with approximate coefficients 0.43, 0.75, 0.97 and 1.31.

To find the Hellinger distance $H_{\min}(f_{b^*})$ from the symmetric class, we need

$$\int_0^1 \sqrt{f_b^*(u)f_b^*(1-u)} \, du = b^* B\left(\frac{b^*+1}{2}, \frac{b^*+1}{2}\right) = \frac{\Gamma^2\left(\frac{b^*+1}{2}\right)}{\Gamma(b^*)}.$$

This quantity approaches $\pi/4$ as $b^* \rightarrow 2$, and using (12) the minimum Hellinger distance to a symmetric distribution approaches $\sqrt{1 - \sqrt{(1 + \pi/4)/2}} = 0.2348882$. The ratio $|\gamma_1(b^*)|/H_{\min}(f_{b^*}) \rightarrow 0.415228$ as $b^* \rightarrow 2$, a value not far from the gradient 0.43 fitted to the 10 models in Figure 6. The ratio $|\gamma_1(b^*)|/H_{\min}(f_{b^*})$ is indeed greater than 0.37 for $b^* > 1$, but for $b^* \leq 2/3$ this ratio falls below $1/3$.

4.3 Classification by tail-weight

We focus on the right-hand tails, leaving the obvious adjustments for left-hand tails to the reader. Let $(f^*)^{(0)}(1) \equiv f^*(1) = \lim_{u \uparrow 1} f^*(u)$, and further for $n \geq 1$ define $(f^*)^{(n)}(1) \equiv \lim_{u \uparrow 1} (f^*)^{(n)}(u)$, assuming these derivatives exist as finite numbers for u near one and their limits as u approaches one exist as finite or infinite values.

Definition 5 Let n^* be the smallest integer $n \geq 0$ for which $(f^*)^{(n)}(1) \neq 0$. If n^* exists, the right tail is of n^* -order; otherwise it is of infinite $*$ -order. For $n^* = 0, 1, 2$ the right tail is called short, medium (exponential) and long respectively. If $n^* \geq 3$ or, then we have ‘very long’ tails.

This definition is consistent with the classification into short, medium and long tails defined by Parzen (1979), provided one combines ‘very long’ with ‘long’. A sampling of examples is in Table 4. Note that for medium tails (the case $n^* = 1$), one has $(f^*)(1) = 0$ and $(f^*)'(1) \neq 0$, but this derivative at 1 must be non-positive. The larger the magnitude $|(f^*)'(1)|$, the shorter the tail. Similarly for long-tailed pdQs, (the case $n^* = 2$), one has $(f^*)(1) = (f^*)'(1) = 0$ and $(f^*)''(1) \neq 0$. Now $(f^*)'(u) \leq 0$ for u near 1, so its derivative $(f^*)''(1)$ will be non-negative or $+\infty$.

The pdQs are only *partially* ordered because different pdQs, such as the normal and Tukey with $0 < \lambda < 1$ can take on the same infinite limit. One could order such pdQs by comparing the ratio of their derivatives $(f^*)'(u)/(g^*)'(u)$ as $u \rightarrow 1$, and similarly for distributions with long or very long tails, but we do not do this here.

The symmetric Tukey(λ) distributions.

The Tukey(λ) family provides a wide range of tail-weights. Starting with f_λ^* from Table 1, the first two derivatives are:

$$\begin{aligned} \kappa_\lambda f_\lambda^*(u) &= \{u^{\lambda-1} + (1-u)^{\lambda-1}\}^{-1} \\ \kappa_\lambda (f_\lambda^*)'(u) &= (1-\lambda)(\kappa_\lambda f_\lambda^*(u))^2 \{u^{\lambda-2} - (1-u)^{\lambda-2}\} \\ \kappa_\lambda (f_\lambda^*)''(u) &= 2(1-\lambda)^2 \frac{\{u^{\lambda-2} - (1-u)^{\lambda-2}\}^2}{\{u^{\lambda-1} + (1-u)^{\lambda-1}\}^3} + (1-\lambda)(\lambda-2) \frac{\{u^{\lambda-3} + (1-u)^{\lambda-3}\}}{\{u^{\lambda-1} + (1-u)^{\lambda-1}\}^2} \\ &\sim 2(1-\lambda)^2 \frac{\{1 - (1-u)^{\lambda-2}\}^2}{\{1 + (1-u)^{\lambda-1}\}^3} + (1-\lambda)(\lambda-2) \frac{\{1 + (1-u)^{\lambda-3}\}}{\{1 + (1-u)^{\lambda-1}\}^2}, \end{aligned}$$

as $u \rightarrow 1$. From the first equation above $f_\lambda^*(1) > 0$ if and only if $\lambda \geq 1$ and in this case $n^* = 0$ and short tails are obtained. For $\lambda < 1$ examination of the first derivative $(f_\lambda^*)'(u)$ as $u \uparrow 1$ yields the value 0 for $\lambda < 0$, the value -6 for $\lambda = 0$ and $-\infty$ for $0 < \lambda < 1$; in these last two cases $n^* = 1$ and the tails are medium (exponential). For $\lambda < 0$ one can see from the last displayed expression that $(f_\lambda^*)''(1) = 0$ when $\lambda < -1$ and we have very long tails. For $-1 \leq \lambda < 0$ $(f_\lambda^*)''(1) > 0$ and we have long tails. In particular, for $\lambda = -1$ the 2nd derivative at 1 is $(f_\lambda^*)''(1) \approx 33.7$ which is not far from that of the Cauchy $4\pi^2$, see Table 4.

Table 4: **Right-tail behavior of some standard continuous distributions.** The pdQs are listed in Table 1. Note that if $f^*(1) = 0$, then $(f^*)'(1) \leq 0$, so its negative is shown in Column 4.

| tail | F | $f^*(1)$ | $-(f^*)'(1)$ | $(f^*)''(1)$ |
|-------------|---|---------------------------------------|--------------|--------------|
| Short | Power(b), $1/2 < b$ | $(2 - 1/b)$ | - | - |
| | Tukey(λ), $1 \leq \lambda \leq 2$ | $\approx 2/\lambda$ | - | - |
| | Tukey(λ), $2 \leq \lambda$ | $\approx (\frac{\pi}{2})^{\lambda-2}$ | - | - |
| Exponential | Normal | 0 | $+\infty$ | - |
| | Tukey(λ), $0 < \lambda < 1$ | 0 | $+\infty$ | - |
| | Logistic (Tukey(0)) | 0 | 6 | - |
| | Extreme Value | 0 | 4 | - |
| | Laplace | 0 | 2 | - |
| | Exponential | 0 | 2 | - |
| Long | Pareto(a), $1 < a$ | 0 | 0 | $+\infty$ |
| | Lognormal | 0 | 0 | $+\infty$ |
| | Tukey(λ), $-1 < \lambda < 0$ | 0 | 0 | $+\infty$ |
| | Cauchy | 0 | 0 | $4\pi^2$ |
| | Tukey(-1) | 0 | 0 | 33.69 |
| | Pareto(1) | 0 | 0 | 6 |
| Very long | Tukey(λ), $\lambda < -1$ | 0 | 0 | 0 |
| | Pareto(a), $0 < a < 1$ | 0 | 0 | 0 |

The lognormal distribution.

The lognormal pdQ is from Table 1 given by $f^*(u) = c \varphi(z_u) \exp(-z_u)$, where $z_u = \Phi^{-1}(u)$ and $c = 1/\kappa = 2\sqrt{\pi} \exp(-0.25)$. Thus $(f^*)'(u) = -c \exp(-z_u)(1 + z_u)$, which approaches 0 as $u \rightarrow 1$. Further, $(f^*)''(u) = c z_u \exp(-z_u)/\varphi(z_u)$, which approaches $+\infty$ as $u \rightarrow 1$ so the lognormal distribution has a long right tail.

The Student-t distribution with $\nu = 2$ degrees of freedom.

The pdQ of Student's distribution with 2 degrees of freedom is $f^*(u) = fQ(u)/\kappa = \{2u(1-u)\}^{3/2}/\kappa$, where the normalizing constant $\kappa = 0.20826$. The reader can readily verify that $f^*(1) = 0$, $(f^*)'(1) = 0$ and $(f^*)''(1) = +\infty$ so this f^* has long tails, but shorter than those of the Cauchy distribution. The tail behavior for large ν may possibly be found using results in Schlüter & Fischer (2012).

The Pareto distributions.

The Pareto(a) family, with $a > 0$ has $f_a^*(u) = (2 + \frac{1}{a})(1-u)^{1+1/a} \rightarrow 0$ as $u \rightarrow 1$. So $(f_a^*)'(u) = -(1 + \frac{1}{a})(2 + \frac{1}{a})(1-u)^{1/a} \rightarrow 0$ as $u \rightarrow 1$, again, for all $a > 0$. Therefore $n^* \geq 2$ and the right-hand tails are always 'long' or 'very long'. The second derivative satisfies, as $u \rightarrow 1$

$$\begin{aligned}
 (f_a^*)''(u) &= \frac{(1+a)(1+2a)}{a^3} (1-u)^{1/a-1} \\
 &\rightarrow \begin{cases} 0, & 0 < a < 1 \\ 6, & a = 1 \\ +\infty, & 1 < a \end{cases}
 \end{aligned}$$

Therefore the tails are long ($n^* = 2$) if and only if $a \geq 1$ and otherwise they are very long ($n^* \geq 3$). Further, one can readily see that $(f_a^*)^{(n)}(1) = 0$ for $0 < a < 1/2^{n-1}$ for all $n \geq 2$. Thus there exist distributions with tails of every n^* -order.

5 Divergence from, convergence to, uniformity

How far is an arbitrary pdQ f^* from uniformity? One approach is to evaluate and plot the Kullback-Leibler divergences from uniformity. Metric comparisons will be made in later sections.

5.1 Divergence from uniformity

Definition 6 Given f_1, f_2 with associated pdQs f_1^*, f_2^* , the square root of the KLD defined in (11) is

$$d^*(f_1, f_2) = \sqrt{J^*(1, 2)} = \sqrt{I^*(1 : 2) + I^*(2 : 1)} .$$

This d^* is not a metric on the space of distributions with pdQs because it does not satisfy the triangle inequality: for example, if \mathcal{U}, \mathcal{N} and \mathcal{C} denote the uniform, normal and Cauchy location-scale families, then $d^*(\mathcal{U}, \mathcal{N}) = 0.5$, $d^*(\mathcal{N}, \mathcal{C}) = 0.4681$ but $d^*(\mathcal{U}, \mathcal{C}) = 1$. However, it can provide a useful measure of distance from uniformity.

Introducing the coordinates $(s_1, s_2) = (\sqrt{I^*(\mathcal{U} : 2)}, \sqrt{I^*(2 : \mathcal{U})})$, we can define the distance from uniformity of any f_2 with associated pdQ f_2^* by the Euclidean distance of (s_1, s_2) from the origin $(0, 0)$, namely $d^*(\mathcal{U}, f_2)$.

These distances from uniformity are easily computed, for using (11) and $f_2^*(u) = (f_2 Q_2)(u)/\kappa_2$ one can write

$$\begin{aligned} I^*(\mathcal{U} : 2) &= - \int_0^1 \ln(f_2^*(u)) du = \ln(\kappa_2) - \int_0^1 \ln\{f_2 Q_2(u)\} du \\ I^*(2 : \mathcal{U}) &= \int_0^1 \ln(f_2^*(u)) f_2^*(u) du = \frac{1}{\kappa_2} \int f_2 Q_2(u) \ln(f_2 Q_2(u)) du - \ln(\kappa_2) . \end{aligned} \quad (14)$$

As explained earlier after (11), $I^*(\mathcal{U} : 2)$ is the mean evidence in one observation $U \sim \mathcal{U}$ for uniformity over f_2^* . Similarly $I^*(2 : \mathcal{U})$ is the mean evidence in one observation $V \sim f_2^*$ for f_2^* over \mathcal{U} .

In Figure 7 are shown the loci of points (s_1, s_2) for several parametric families. The light dotted arcs with radii 1/2, 1 and 2 mark the d^* distance from uniformity. The large discs in (purple, red and black) correspond to \mathcal{U}, \mathcal{N} and \mathcal{C} . The chi-squared(ν), $\nu > 1$, family appears as red curve; the Weibull(β), for $0.5 \leq \beta \leq 15$ in blue; it crosses the exponential locus (blue cross) when $\beta = 1$.

The top green line corresponds to Tukey(λ) with $2 \leq \lambda \leq 15$; it also has a lower green curve emanating from the origin for $\lambda < -1$ which is hidden but close to the Pareto(a) curve $1/4 \leq a$ curve shown in black, but ending in the exponential blue cross as $a \rightarrow \infty$. Nearby is the lognormal point (red cross). The lower Tukey(λ) curve is partially hidden by the swathe of green GLD(λ_3, λ_4) points, with each parameter varying from -5 to 15 . The blue swathe of points corresponds to Beta(a, b) pdQs with $0.5 < a, b \leq 5$.

Many more loci for different families could be plotted, but are omitted for the sake of clarity. For U-shaped distributions such as the B(a, b) with $1/2 < a, b < 1$ and many other short tailed distributions, $I^*(2 : \mathcal{U}) > I^*(\mathcal{U} : 2)$, and the corresponding points on the map are above the main diagonal. However the longer tailed distributions are located below it.

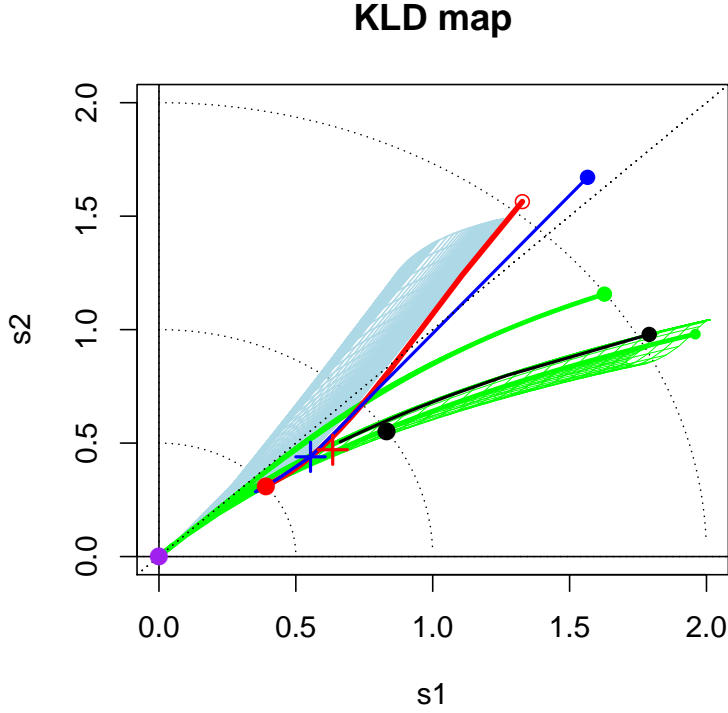


Figure 7: **Divergence from uniformity.** The loci of points $(s_1, s_2) = (\sqrt{I^*(U : 2)}, \sqrt{I^*(2 : U)})$ defined in (14) is shown for various standard families. The large disks correspond, respectively to the symmetric families uniform (purple), normal (red) and Cauchy (black). The crosses correspond to the asymmetric distributions exponential (blue) and lognormal (red). The solid red curve is the locus of points defined by the Chi-squared family with degrees of freedom $\nu > 1$; this curve begins at the red circle and proceeds towards the normal point, as $\nu \rightarrow \infty$. The solid green curves emanating from the origin are the points corresponding to the Tukey(λ) family; the lower line is for $\lambda < 1$; the upper for $\lambda \geq 1$. The solid black curve is the locus of points defined by the Pareto family with shape parameter $a > 1/4$; it approaches the exponential (blue cross) as $a \rightarrow \infty$. The light blue swathe of points corresponds to Beta distributions and the light-green swathe to the generalized Tukey distributions; more details are given in Section 5.1.

5.2 Examples of convergence to uniformity

The transformation $f \rightarrow f^*$ of Definition 1 is quite powerful, being location-scale invariant and moving the distribution from the support of f to the unit interval. What happens with another application of the transformation to $f^{**} = (f^*)^*$? And further, with n iterations $f^{(n+1)*} = (f^{n*})^*$ for $n \geq 2$, and $n \rightarrow \infty$? An R script Team (2008) for finding repeated $*$ -iterates of a given pdQ is in Appendix 7.2

Example 1: Power function family.

From Table 1 the Power(b) family has density $f_b(x) = bx^{b-1}$, $0 < x < 1$, quantile function $Q_b(u) = u^{1/b}$ and, if $b > 1/2$, so that $b^* = (2b - 1)/b > 0$, the pdQ $f_b^*(u) = b^*u^{b^*-1}$. This f_b^* has $F_b^*(u) = u^{b^*}$ and quantile function $Q_b^*(u) = u^{1/b^*}$. Hence, for $b > 2/3$, and $b^{**} = (3b - 2)/(2b - 1) > 0$, the pdQ f_b^{**} exists. It is given by $f_b^{**}(u) = b^{**}u^{b^{**}-1}$. In general, f_b^{n*} exists and is in the Power(b) family only if $b > n/(n+1)$ and then $b^{n*} = \{(n+1)b - n\}/(nb - n + 1)$. Therefore for any $b < 1$ the sequence $\{f_b^{n*}\}$ is finite, while for $b = 1$ all elements are uniform, and for $b > 1$ we have $b^{n*} \rightarrow 1$ so the elements f_b^{n*} converge to the uniform.

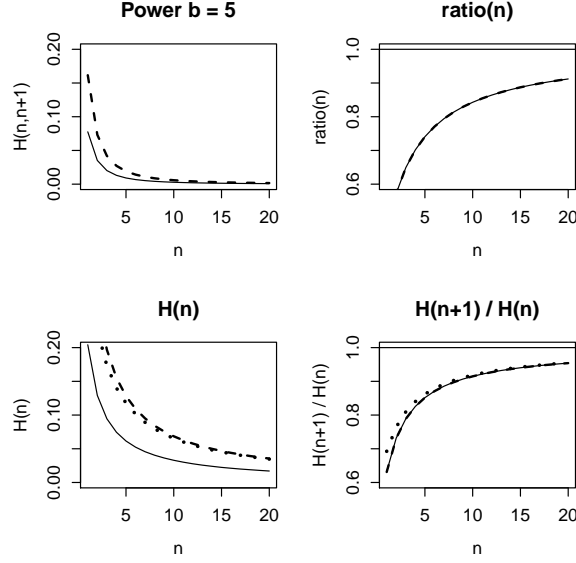


Figure 8: **Power density $f(b^{n*})$ convergence, where $b = 5$:** The upper left plot shows $H(n, n+1)$ of Definition 7 in solid lines and $L(n, n+1)$ in dashed lines, plotted as functions of n . The upper right plot shows the corresponding ratios $r_H(n) = H(n+1, n+2)/H(n, n+1)$ of Hellinger distances of adjacent members of the sequence as a function of n ; they are the same as for the L_1 distance ratios. In the lower left plot are shown the Hellinger distances $H(n)$ of $f(b^{n*})$ from the uniform distribution, again as a solid line, together with the L_1 distances $L(n)$ as dashed line. The dotted line is a plot of the asymptotic approximation for $L(n)$ found in (16). The bottom right plot depicts the ratio of successive distances from the uniform as n increases; note that the ratios again agree for Hellinger and L_1 metrics. Finally, the dotted line shows the asymptotic expression for these distances (17).

Definition 7 Let $H(f, g)$ be the Hellinger distance of f from g given in (10). Given any sequence $\{f^{n*}\}$ of successive pdQs generated by a pdQ f^* and successive $*$ -maps, define $H(n, n+1) = H(f^{n*}, f^{(n+1)*})$ and $H(n) = H(f^{n*}, \mathcal{U})$, for $n = 1, 2, \dots$. Similarly for the L_1 distance on the unit interval $\|f - g\|_1 = \int_0^1 |f(u) - g(u)| du$, introduce $L(n, n+1) = \|f^{n*} - f^{(n+1)*}\|_1$ and $L(n) = \|f^{n*} - \mathcal{U}\|_1$.

Usually we resort to numerical integration to determine $H(n, n+1)$, $H(n)$, $L(n, n+1)$ and $L(n)$, but in some cases it is possible to find exact expressions for them. For example, to find the L_1 -distance of $\{f_b^{n*}\}$ to \mathcal{U} , define $a = b^{1/(1-b)}$ and evaluate

$$\begin{aligned} L_b(1) &= \int_0^1 |f_b(u) - 1| du = \int_0^a (1 - f_b(u)) du + \int_a^1 (f_b(u) - 1) du \\ &= 2a(1 - a^{b-1}) = 2 \left(1 - \frac{1}{b}\right) b^{1/(1-b)}. \end{aligned} \quad (15)$$

Therefore, writing $b^{n*} = 1 + \{n + c\}^{-1}$, where $c = (b - 1)^{-1}$,

$$L_b(n) = 2 \frac{1}{n + c + 1} \left(1 + \frac{1}{n + c}\right)^{-(n+c)} \sim \frac{2}{e\{n + b/(b-1)\}}. \quad (16)$$

Further

$$L_b(n+1)/L_b(n) \sim \frac{\{n + b/(b-1)\}}{\{n + 1 + b/(b-1)\}} \sim 1 - \frac{e L_b(n+1)}{2}. \quad (17)$$

As an example, fix the sequence $\{f_b^{n*}\}$ for $b = 5$. Figure 8 contains plots showing (in solid lines, top left) the successive Hellinger distances $H(n, n+1)$; top right, the ratios $r_H(n) = H(n+1, n+2)/H(n+1, n)$; bottom left, the distances from

uniformity $H(n)$; and bottom right, the ratios of such distances $H(n+1)/H(n)$. Superimposed in dashed lines are the corresponding values and ratios for the L_1 metric. Remarkably the ratios are same for these two metrics.

An important consequence of this example is that convergence to uniformity is order $1/n$ for each metric, and further with $H(n+1)/H(n) = L(n+1)/L(n) \uparrow 1$. It is also worth noting that the ratios of distances of successive members also approaches one, precluding either metric leading to a contraction map on the Banach space $L_1[0, 1]$ of Lebesgue integrable functions on $[0, 1]$.

Example 2: Exponential distribution.

Suppose $f(x) = e^x$, $x < 0$. Then $f^*(u) = 2u$, $0 < u < 1$ which belongs to the Power(2) distribution, and so by Example 1, f^{n*} converges to the uniform distribution as $n \rightarrow \infty$. By symmetry, the same result holds for $f(x) = e^{-x}$, $x > 0$.

Example 3: Pareto distribution.

The Pareto(a) family, with $a > 0$ has $f_a^*(u) = (2 + \frac{1}{a})(1 - u)^{1+1/a}$. Therefore $F_a^*(u) = (1 - u)^{2+1/a}$, $Q_a^*(u) = 1 - u^{a/(1+2a)}$ and $f_a^{**}(u) = \frac{(2+3a)}{(1+2a)} u^{(1+a)/(1+2a)}$, which is in the Power(b) family, with $b = \frac{(2+3a)}{(1+2a)} > 1$ for all $a > 0$, so by Example 1, the sequence $\{f_a^{n*}\}_{n \geq 1}$ exists and converges to the uniform distribution as $n \rightarrow \infty$.

Example 4: Cauchy distribution.

The pdQ of the Cauchy density is given by $f^*(u) = 2 \sin^2(\pi u)$, $0 < u < 1$, see Table 2; it retains the bell shape of f as shown in Figure 1. It follows that $F^*(t) = t - \sin(2\pi t)/(2\pi)$, for $0 < t < 1$. To obtain f^{**} , one needs to solve numerically for Q^* , numerically compute $\kappa^* = \int_0^1 (f^* Q^*)(u) du$ and then $f^{**}(u) = (f^* Q^*)(u)/\kappa^*$. A plot of f^{**} (not shown) reveals its shape is close to that of φ^* , the pdQ of the normal. Thus two iterations of the $*$ -operation is required to remove the bell-shape of the original Cauchy, and bring it closer to that of the single operation on φ .

Example 5: Normal distribution.

The pdQ of the normal density is $\varphi^*(u) = 2\sqrt{\pi} \varphi(z_u)$, where $z_u = \Phi^{-1}(u)$. Thus its distribution function is

$$\Phi^*(u) = 2\sqrt{\pi} \int_{-\infty}^{z_u} \varphi^2(x) dx = \frac{1}{\sqrt{\pi}} \int_{-\infty}^{z_u} e^{-x^2} dx = \int_{-\infty}^{z_u} \sqrt{2} \varphi(\sqrt{2}x) dx = \Phi(\sqrt{2}z_u).$$

The quantile function $Q^*(t) = (\Phi^*)^{-1}(t)$ is the solution z_t^* to $t = \Phi(\sqrt{2}\Phi^{-1}(z_t^*))$; it is $z_t^* = Q^*(t) = \Phi(z_t/\sqrt{2})$. Hence the density quantile function of φ^* is $\varphi^*(Q^*(u)) = 2\sqrt{\pi} \varphi(z_u/\sqrt{2})$, $\kappa^* = 2\sqrt{\pi} \int_0^1 \varphi(z_u/\sqrt{2}) du = 2/\sqrt{3}$, and $\varphi^{**}(u) = \sqrt{3\pi} \varphi(z_u/\sqrt{2})$. Continuing, one can show by induction that $\varphi^{n*}(u) = \sqrt{1+1/n} \sqrt{2\pi} \varphi(z_u/\sqrt{n})$. Therefore, for any $0 < u < 1$ we have $\varphi^{n*}(u) \rightarrow 1$ as $n \rightarrow \infty$. An analysis and plots (not shown) of the rates of convergence of $\{\varphi^{n*}\}$ like those in Figure 8 for $\{f_5^{n*}\}$ was carried out with similar results, although we did not attempt to find asymptotic expression such as (16) and (17). These examples suggest to us that for bounded densities, repeated application of the $*$ -transformation will lead to uniformity. Even weaker conditions may suffice.

5.3 Conditions for convergence to uniformity

Definition 8 Given $f \in \mathcal{F}'$, we say that f is of $*$ -order n if $f^*, f^{2*}, \dots, f^{n*}$ exist but $f^{(n+1)*}$ does not. When the infinite sequence $\{f^{n*}\}_{n \geq 1}$ exists, it is said to be of infinite $*$ -order.

For example, the Power(3/4) family is of $*$ -order 2, while the Power(2) family is of infinite $*$ -order. The χ_ν^2 distribution is of finite $*$ -order for $1 < \nu < 2$ and infinite $*$ -order for $\nu \geq 2$. The normal distribution is of infinite $*$ -order.

Next we investigate the involutory nature of the $*$ -transformation.

Lemma 1 Let f^* be a pdQ with quantile function Q^* , and assume f^{**} exists. Then $f^* \sim \mathcal{U}$ if and only if $f^{**} \sim \mathcal{U}$.

Proof of Lemma : By definition $f^{**}(u) = f^*Q^*(u)/\kappa^*$, where $\kappa^* = \int_0^1 (f^*)^2(u) du$. If $f^*(u) \equiv 1$, then $F^*(u) \equiv u \equiv Q^*(u)$, so $\kappa^* = 1$ and $f^{**}(u) \equiv u$.

Conversely, if $f^{**}(u) \equiv 1$, then $f^*Q^*(u) \equiv \kappa^*$ and the quantile density $q^*(u) \equiv 1/\kappa^*$. It follows that the quantile function $Q^*(u) \equiv u/\kappa^* + c$ for some real c , and hence that $F^*(v) = \kappa^*(v - c)$ for $0 \leq v \leq 1$. But f^* is a pdQ, having distribution F^* satisfying $F^*(0) = 0$ and $F^*(1) = 1$. These conditions imply $-c\kappa^* = 0$ and $\kappa^*(1 - c) = 1$, or $c = 0$ and $\kappa^* = 1$. Thus $f^* \sim \mathcal{U}$, as required.

Proposition 2 Given $f \in \mathcal{F}'$, either f the infinite sequence $\{f^{n*}\}_{n \geq 1}$ exists if and only if $\int f^n(x) dx < \infty$ for all $n \geq 2$.

The proof of Proposition 2 is in the Appendix 7.2

We conjecture that if $\{f^{n*}\}_{n \geq 1}$ exists, then the sequence converges to the uniform distribution on the unit interval. Note that Lemma 1 shows that the uniform distribution is a fixed point in the Banach space of integrable functions on $[0,1]$ with the L_1 -norm. It remains to show f^{n*} has a limit and that the limit is the uniform distribution. It was hoped the classical machinery for convergence in Banach spaces (Luenberger, 1969, Ch.10) would prove useful in this regard, but the $*$ -mapping is not a contraction, as shown by Example 1 of Section 5.2.

6 Summary and Discussion

Given that a pdQ f^* exists for a continuous distribution with density f , then so does F^* and Q^* . Thus a monotone transformation from $X \sim F$ to $X^* \sim F^*$ exists; it is simply $X^* = m(X) = Q^*(F(X))$. For the Power(b) distribution, $m_b(x) = Q_b^*(F_b(x)) = x^{b/b^*} = x^{b^2/(2b-1)}$. For the normal distribution with parameters μ, σ , it is $m_{\mu, \sigma}(x) = \Phi((x - \mu)/\sqrt{2}\sigma)$. Unfortunately, in general there does not seem to be any explicit expression for Q^* that depends only on f or F .

The pdQ transformation from f to f^* allows for a different look at distributional shapes, on a common finite domain $[0,1]$ where location, scale and gaps are not distractions. For such f^* we can find moments of all orders, and because the support is compact, such moments determine the pdQ.

While the pdQs of discrete distributions are of interest, we have not delved into them much here. For example, the moments in Table 1 could include those of discrete distributions. The KLD map in Figure 7 for continuous distributions could have included discrete distributions. It would also be of interest to extend the tail-weight analysis of Section 4.3 to discrete distributions, although the boundary derivatives could not be found as limits of derivatives near the boundary.

With regard to right tail-weight, those pdQs of n^* -order, but infinite n^* derivative at 1, could be compared by looking at the relative rates at which these n^* derivatives approach infinity. It would be of interest to include the Student- $t\nu$ pdQs for $\nu > 1$ degrees of freedom and many other long and very long tailed distributions in Table 4. Another unresolved problem is whether convergence to uniformity holds under the weak condition stated at the end of Section 5.3.

We have not discussed data analysis and inference, except to provide empirical estimators for continuous and discrete pdQs, but we think that the location-, scale- and gap-free pdQ empirical plots will make it easier to compare shapes of one-dimensional distributions. A more ambitious task is to extend these results to the bivariate or even multivariate case.

References

- EPANECHNIKOV, V.A. 1969. Nonparametric estimation of a multivariate probability density. *Theory of Probability and its Applications*, **14**, 153–158.
- FALK, M. 1986. On the estimation of the quantile density function. *Statistics and Probability Letters*, **4**, 69–73.
- FREIMER, M., MUDHOLKAR, G.S., KOLLIA, G., & LIN, C.T. 1988. A study of the generalized tukey lambda family. *Communications in Statistics - Theory and Methods*, **17**, 3547–3567.
- GILCHRIST, W. 2000. *Statistical modelling with quantile functions*. London: Chapman and Hall/CRC.
- JOHNSON, N.L., KOTZ, S., & KEMP, A.W. 1993. *Univariate discrete distributions*. second edn. New York: John Wiley & Sons.
- JOHNSON, N.L., KOTZ, S., & BALAKRISHNAN, N. 1994. *Continuous univariate distributions*. Vol. 1. New York: John Wiley & Sons.
- JOHNSON, N.L., KOTZ, S., & BALAKRISHNAN, N. 1995. *Continuous univariate distributions*. Vol. 2. New York: John Wiley & Sons. ISBN 0-471-58494-0.
- JONES, M.C. 1992. Estimating densities, quantiles, quantile densities and density quantiles. *Annals of Institute of Statistical Mathematics*, **44**(4), 721–727.
- KULLBACK, S. 1968. *Information theory and statistics*. Mineola, NY: Dover.
- LUENBERGER, D.G. 1969. *Optimization by Vector Space Methods*. New York, NY: Wiley.
- MA, Y., GENTON, M.G., & PARZEN, E. 2011. Asymptotic properties of sample quantiles of discrete distributions. *Annals of the Institute of Statistical Mathematics*, **63**, 227–243.
- PARZEN, E. 1979. Nonparametric statistical data modeling. *Journal of the American Statistical Association*, **7**, 105–131.
- PARZEN, E. 2004. Quantile probability and statistical data modeling. *Statistical Science*, **4**, 652–662.
- PRENDERGAST, L.A., & STAUDTE, R.G. 2016. Exploiting the quantile optimality ratio in finding confidence intervals for a quantile. *Stat*, **5**(1), 70–81.
- SCHLÜTER, S., & FISCHER, M. 2012. A tail quantile approximation for the student t distribution. *Communications in statistics: Theory and methods*, **41**(15), 2617–2625.
- STAUDTE, R.G. 2014. Inference for quantile measures of skewness. *Test*, **23**(4), 751–768.

- TEAM, R DEVELOPMENT CORE. 2008. *R: A language and environment for statistical computing*. R Foundation for Statistical Computing, Vienna, Austria. ISBN 3-900051-07-0.
- TUKEY, J.W. 1962. The future of data analysis. *Annals of Mathematical Statistics*, **33**, 1–67.
- TUKEY, J.W. 1965. Which part of the sample contains the information? *Proceedings of the Mathematical Academy of Science USA*, **53**, 127–134.
- TUKEY, J.W. 1977. *Exploratory Data Analysis*. Reading, MA: Addison-Wesley.
- WELSH, A.H. 1988. Asymptotically efficient estimation of the sparsity function at a point. *Statistics and Probability Letters*, **6**, 427–432.
- WITHERS, C.S., & NADARAJAH, S. 2010. Methods for symmetrizing random variables. *Probability in the Engineering and Informational Sciences*, **24**, 549–559.

7 Appendix

7.1 Proof of Proposition 1

Proof of Proposition 1. Part (a) is Theorem 2.2 of Withers & Nadarajah (2010). Part (b) is a straightforward modification of the proof of Part(a): let X have a distribution on the integers with $P(X = i) = p_i$ and let Y be a symmetric distribution on the integers with $P(Y = i) = q_i$, so $q_{-i} = q_i$, $i \geq 1$. Amongst such q we will minimize the divergence $I(p : q) = \sum_i p_i \ln(p_i/q_i) = \sum_i p_i \ln(p_i) - p_0 \ln(q_0) - \sum_{i=1}^{\infty} (p_i + p_{-i}) \ln(q_i)$. Taking λ as a Lagrange multiplier, we need to solve $0 \equiv \frac{\partial}{\partial q_i} \{I(p : q) + \lambda \sum_i q_i\}$. This yields $0 = -p_0/q_0 + \lambda$ and $0 = -(p_i + p_{-i})/q_i + 2\lambda$ for $i > 0$. Therefore $q_0 = p_0/\lambda$ and $q_i = (p_i + p_{-i})/(2\lambda)$. The condition $\sum_i q_i = 1$ then implies $\lambda = 1$. Thus $q_i = (p_i + p_{-i})/2$ for all i .

Clearly this result can be extended to an arbitrary discrete distribution on a lattice of points $\mathcal{X} = \{x_i\}$ by extending \mathcal{X} to $\mathcal{X} \cup -\mathcal{X}$, letting $P(X = x_i) = p_i$ and using the same argument. The absolutely continuous case then follows by approximating the density over a lattice with smaller and smaller increments and taking the limit.

For part (c), again return to a given discrete distribution p on the integers, and a symmetric distribution q on the integers. For each positive integer i introduce $2a_i = \ln(p_i p_{-i})$ and $\nu_i = \sqrt{p_i p_{-i}} = \exp(a_i)$. Further let $\bar{p}_i = (p_i + p_{-i})/2$. To minimize the KLD between p and q by choice of symmetric q we need to minimize

$$J(p, q) = \sum_i p_i \ln(p_i) - p_0 \ln(q_0) - 2 \sum_{i=1}^{\infty} \bar{p}_i \ln(q_i) + q_0 \ln(q_0/p_0) + 2 \sum_{i=1}^{\infty} q_i (\ln(q_i) - a_i) .$$

Setting the derivatives $0 \equiv \frac{\partial}{\partial q_i} \{J(p, q) + \lambda \sum_i q_i\}$ yields $0 = -p_0/q_0 + \ln(q_0/p_0) + 1 + \lambda$ and $0 = 2\{-\bar{p}_i/q_i + \ln(q_i) - a_i + 1 + \lambda\}$ for $i > 0$. The solution for q is implicit in:

$$\begin{aligned} q_0 &= p_0 \exp\{p_0/q_0\} e^{-\lambda-1} ; \\ q_i &= \nu_i \exp\{\bar{p}_i/q_i\} e^{-\lambda-1} , \text{ for } i \geq 1 ; \\ 1 &= q_0 + 2 \sum_{i=1}^{\infty} q_i . \end{aligned} \tag{18}$$

As in parts (a) and (b), the proof of part (c) is completed by a limiting argument.

Algorithm for computing the solution to (18).

Given a discrete distribution p , \mathcal{X} , one may solve the equations (18) iteratively. For the continuous case we solved the equations (13) as follows:

1. Given f_1 compute $\nu(x) = \sqrt{f_1(x)f_1(-x)}$ and $\bar{f}_1(x) \equiv \{f_1(x) + f_1(-x)\}/2$.
2. Fix $C = e^{-\lambda-1} > 0$ and for each x in a fine grid over the support of f_1 solve for $\beta(x; C)$

$$\beta(x) = \nu(x) \exp \{ \bar{f}_1(x) / \beta(x) \} C .$$

Numerically compute $d_C = \int \beta(x; C) dx$, normalize $\beta(x; C)$ to a probability density $f_2(x; C) = \beta(x; C)/d_C$ and use it to calculate $J(1, 2; C)$.

3. Repeat the last step for a range of C values to locate the $C = C_{opt}$ for which $J(1, 2; C)$ is minimized. This $f_2(x; C_{opt})$ is the solution guaranteed by (13).

Examples of computing (18). In the left plot of Figure 9 are shown the symmetric densities closest to the lognormal pdQ (in minimizing the divergences $I(1 : 2)$, $I(2 : 1)$ and $J(1, 2)$). Also shown are values $J(1, 2; C) = \int \{f_1(u) \log(f_1(u)/f_C(u)) + f_C(u) \log(f_C(u)/f_1(u))\} du$, where $f_C(u) \equiv f_2(x; C) = \beta(x; C)/d_C$ in the iterative Step 2 above. Figure 10 gives the corresponding results for the Pareto $a = 1$.

7.2 Proof of Proposition 2

Proof of Proposition2: Recall from (2) that f^* exists if and only if $\kappa = \int_0^1 (fQ)(u) du = \int f^2(x) dx$ is finite, and then $f^*(u) \equiv (fQ)(u)/\kappa$. Applying this fact to f^* , f^{**} exists if and only if $\kappa^* = \int_0^1 (f^*)^2(u) du < +\infty$, and then $f^{**}(u) = f^*Q^*(u)/\kappa^*$. This requires, using the change of variable $u = F(x)$,

$$\kappa^* = \int_0^1 \frac{\{(fQ)(u)\}^2}{\kappa^2} du = \frac{1}{\kappa^2} \int f^3(x) dx < +\infty .$$

Assuming f^{**} exists, f^{3*} exists if and only if $\kappa^{**} = \int_0^1 (f^{**})^2(u) du < +\infty$, and then $f^{3*}(u) = f^{**}Q^{**}(u)/\kappa^{**}$. This requires that, with successive changes of variable $u = F^*(v)$, $v = F(x)$

$$\kappa^{**} = \int_0^1 \frac{\{(f^*Q^*)(u)\}^2}{(\kappa^*)^2} du = \frac{1}{(\kappa^*)^2} \int_0^1 (f^*)^3(v) dv = \frac{1}{(\kappa^*)^2 \kappa^3} \int f^4(x) dx < +\infty .$$

The pattern is clear: assuming the course of values inductive hypothesis that $f^*, f^{2*}, \dots, f^{n*}$ exist, which entails the finiteness of $\int f^m(x) dx$ for $m = 2, \dots, n+2$ we can make n successive changes of variable in κ^{n*} to show that it is finite if and only if $\int f^{n+1}(x) dx < +\infty$, and then $f^{(n+1)*}(u) = f^{n*}Q^{n*}(u)/\kappa^{n*}$ exists.

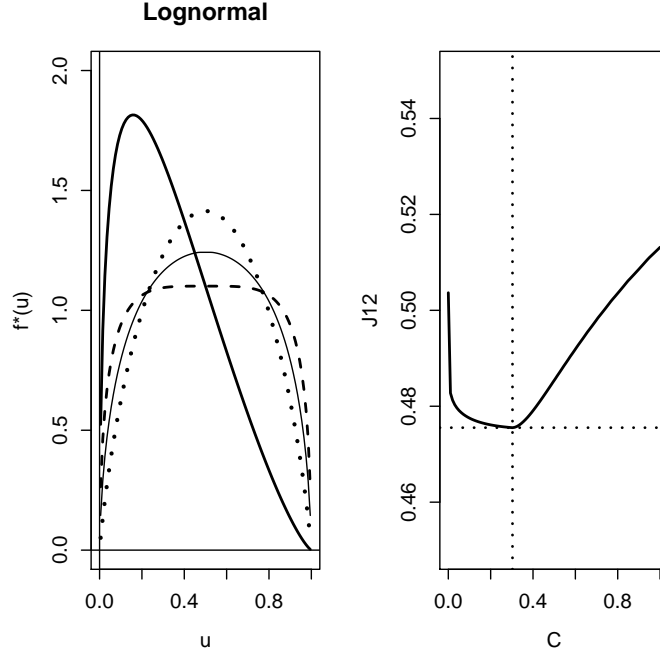


Figure 9: On the left is shown the the lognormal pdQ $f^*(u)$ (thick solid line) and the respective closest symmetric distributions that minimize $I(1:2)$ (dashed line), $I(2:1)$ (dotted line) and $J(1,2)$ (thin solid line). On the right are shown values of $J(1,2;C)$ for various C ; the C_{opt} which minimizes the KLD distance $J(1,2)$ is marked by a vertical line. The closest symmetric density (in the Hellinger metric) to the lognormal pdQ is the same as that minimizing $J(1,2)$.

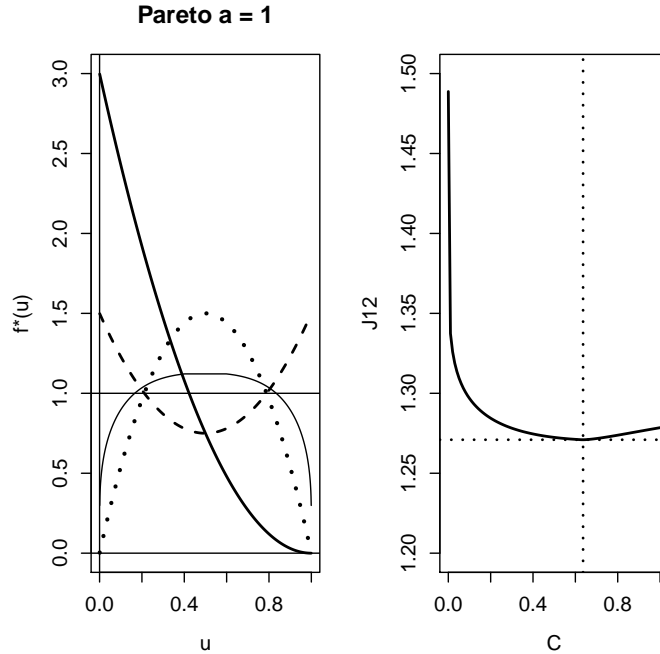


Figure 10: **Pareto with $a = 1$.** Similar results to those in Figure 9. The horizontal line at 1 marks the uniform density, which is the closest (in the Hellinger metric) symmetric density to this Pareto pdQ,